

## Washington University School of Medicine Digital Commons@Becker

---

### Open Access Publications

---

8-30-2004

# Yeast actin patches are networks of branched actin filaments

Michael E. Young

*Washington University School of Medicine in St. Louis*

John A. Cooper

*Washington University School of Medicine in St. Louis*

Paul C. Bridgman

*Washington University School of Medicine in St. Louis*

Follow this and additional works at: [http://digitalcommons.wustl.edu/open\\_access\\_pubs](http://digitalcommons.wustl.edu/open_access_pubs)



Part of the [Medicine and Health Sciences Commons](#)

---

### Recommended Citation

Young, Michael E.; Cooper, John A.; and Bridgman, Paul C., "Yeast actin patches are networks of branched actin filaments." *The Journal of Cell Biology*.166,5. 629-635. (2004).  
[http://digitalcommons.wustl.edu/open\\_access\\_pubs/585](http://digitalcommons.wustl.edu/open_access_pubs/585)

This Open Access Publication is brought to you for free and open access by Digital Commons@Becker. It has been accepted for inclusion in Open Access Publications by an authorized administrator of Digital Commons@Becker. For more information, please contact [engeszer@wustl.edu](mailto:engeszer@wustl.edu).

# Yeast actin patches are networks of branched actin filaments

Michael E. Young,<sup>1</sup> John A. Cooper,<sup>1</sup> and Paul C. Bridgman<sup>2</sup>

<sup>1</sup>Department of Cell Biology and Physiology and <sup>2</sup>Department of Anatomy and Neurobiology, Washington University School of Medicine, St. Louis, MO 63110

Cortical actin patches are the most prominent actin structure in budding and fission yeast. Patches assemble, move, and disassemble rapidly. We investigated the mechanisms underlying patch actin assembly and motility by studying actin filament ultrastructure within a patch. Actin patches were partially purified from *Saccharomyces cerevisiae* and examined by negative-stain electron microscopy (EM). To identify patches in the EM, we correlated fluorescence and EM images of GFP-labeled patches. Patches contained a network of actin filaments with branches

characteristic of Arp2/3 complex. An average patch contained 85 filaments. The average filament was only 50-nm (20 actin subunits) long, and the filament to branch ratio was 3:1. Patches lacking Sac6/fimbrin were unstable, and patches lacking capping protein were relatively normal. Our results are consistent with Arp2/3 complex-mediated actin polymerization driving yeast actin patch assembly and motility, as described by a variation of the dendritic nucleation model.

## Introduction

Budding yeast contain actin binding and regulatory proteins, most of which are found in all eukaryotes, suggesting that fundamental mechanisms of actin dynamics and regulation may be conserved (Pollard and Borisy, 2003). However, the actin concentration is much less in yeast than in vertebrate cells (Nefsky and Bretscher, 1992). The most prominent yeast actin structures are cortical patches (Adams and Pringle, 1984), which have been implicated in endocytosis and cell wall remodeling (Utsugi et al., 2002; Kaksonen et al., 2003). Actin patches are dynamic. They assemble, move, and disassemble within minutes.

Patch formation and movement appear to require actin polymerization nucleated by Arp2/3 complex (Winter et al., 1997). Purified Arp2/3 complex generates end to side branches with a specific angle and polarity (Mullins et al., 1998; Volkman et al., 2001). Arp2/3 complex branches have been observed in cell extracts and detergent-extracted cultured vertebrate cells (Svitkina and Borisy, 1999; Cameron et al., 2001). In situ cryoEM studies of *Dictyostelium* revealed

branched thin filaments, but filament polarity was not determined and many branch angles were not characteristic of Arp2/3 complex (Medalia et al., 2002).

Actin-based motility can be reconstituted with purified Arp2/3 complex, capping protein, and ADF/cofilin (Loisel et al., 1999). This observation and the biochemical and structural studies above have led to the dendritic nucleation model (Pollard and Borisy, 2003), which is proposed to account for actin-based motility in vertebrate cells at the leading edge and comet tails of pathogens such as *Listeria monocytogenes* (Loisel et al., 1999). The dendritic nucleation model may apply to yeast actin patches. Activators of Arp2/3 complex appear to direct the growth and maturation of actin patches (Kaksonen et al., 2003). However, although capping protein colocalizes with Arp2/3 complex at sites of actin assembly in most systems (Wear and Cooper, 2004), and capping protein is a yeast actin patch component, yeast strains lacking capping protein are viable, and their actin patches assemble and move (Kim et al., 2004). In addition, cofilin may be unnecessary for patch motility (Lappalainen and Drubin, 1997). Thus, the dendritic nucleation model may not apply to actin patches.

Actin patch assembly and movement in yeast have been well studied by genetic, cell biological, and biochemical approaches. However, a key piece of the puzzle is missing: how are actin filaments in a patch organized? Ultrastructural studies of the yeast actin cytoskeleton have been challenging because of the high density of yeast cytosol. A thin-section

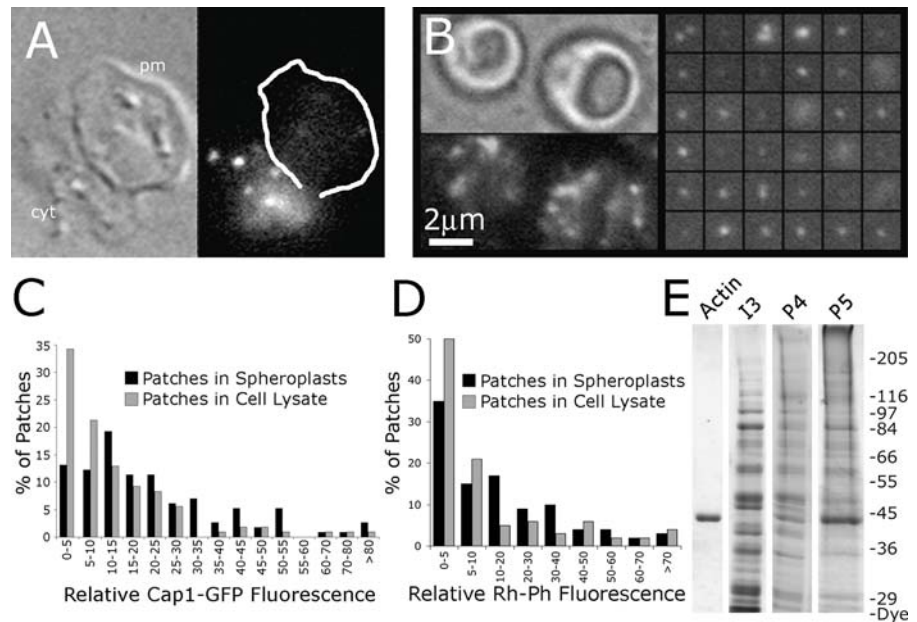
The online version of this article contains supplemental material.

M.E. Young's present address is Concordia University, 1530 Concordia West, Irvine, CA 92612.

Address correspondence to John Cooper, Box 8228, 660 S. Euclid Ave., St. Louis, MO 63110. Tel.: (314) 362-3964. Fax: (314) 362-0098. email: jcooper@wustl.edu

Key words: yeast actin; Arp2/3 complex; dendritic nucleation; electron microscopy; correlation microscopy

**Figure 1. Comparison of isolated actin patches with patches in cells.** (A) A lysed Cap1-GFP spheroplast, strain YJC1453, shows actin patches expelled with the cytoplasm (cyt), not retained on the plasma membrane ghost (pm). (B) Cap1-GFP actin patches in spheroplasts (left) are similar in size and intensity to those in a cell lysate (right). Fluorescence images were collected and displayed with the same settings, allowing one to compare the intensities. (C) Quantitation of the fluorescence intensity of Cap1-GFP labeled patches in B;  $n = 100$ . (D) Quantitation of filamentous actin in patches, by rhodamine-phalloidin,  $n = 100$ . (E) A Coomassie-stained SDS gel of fractions from an actin patch preparation. The cell lysate and fractions up to I3 were indistinguishable. P5 represents the entire contents of one preparation; other lanes are portions of another preparation.



EM study found actin patches at plasma membrane invaginations with filaments around some invaginations (Mulholland et al., 1994). Rapid-freeze, deep-etch EM of the plasma membrane's cytoplasmic face revealed structures containing short actin filaments and several actin-binding patch components (A. Rodal, B. Goode, D. Drubin, and J. Hartwig, personal communications).

In this work, we isolated and partially purified GFP-labeled actin patches and correlated fluorescence and EM images to identify actin patches in the EM. Patches contained networks of branched actin filaments. The network characteristics in wild-type and mutant cells have implications for patch assembly and movement and the applicability of the dendritic nucleation model in yeast.

## Results and discussion

### Purification of actin patches

Actin patches are at the cell cortex, but when yeast are lysed, patches are expelled with the cytoplasm (Fig. 1 A). To purify actin patches, we GFP-labeled them and followed them by fluorescence microscopy. Unless stated otherwise, we GFP-labeled the Cap1 subunit of capping protein. GFP-labeled patches in cell lysates did not correlate with any structures observed with DIC or phase contrast optics and were absent in preparations from strains lacking GFP. Actin patches were stable at 4°C in a concentrated cell lysate for >24 h, but disassembled in <2 h at 25°C or when diluted into a variety of buffers. We found that KS buffer, which contains 1 M sorbitol and 0.2 M potassium phosphate, stabilized patches to dilution for hours. Because patches *in vivo* turn over in minutes, we asked if KS stabilized actin filaments. Pure actin filaments disassembled in <100 s when diluted into control buffers, but only ~5% of actin depolymerized within 10 min when diluted into KS. Phosphate alone prevented depolymerization (Fig. S1, available at <http://www.jcb.org/cgi/content/full/jcb.200404159/DC1>), and it stabilizes Arp2/3 complex-mediated actin branches (Blan-

choin et al., 2000). However, stabilizing actin patches required both phosphate and sorbitol.

If purified patches are to be representative of patches in cells, then the patches and the actin filaments within them must be stable. Most important, there should be no polymerization creating new structures, especially in the cell lysate, where there is a pool of monomeric actin. We quantitated F-actin and capping protein in patches *in vivo* and in the lysate. Rhodamine-phalloidin staining of patches, reflecting F-actin content, decreased ~5% after lysis, whereas Cap1-GFP decreased by ~35%. Patches with increased brightness were not observed (Fig. 1, B–D). Patches labeled with Abp1-GFP or Sac6/fimbrin-GFP gave similar results. Thus, with respect to actin filaments and three actin-binding proteins, patches remained intact through cell lysis, and net actin assembly did not occur in the lysate.

We purified patches by differential centrifugation. A lysate of spheroplasts was cleared with a low speed spin, yielding fraction S1. At this point, the chemical cross-linker glutaraldehyde was usually added to preserve patch structure. Cross-linking was not essential and was omitted for certain experiments as described. A high speed clarification and three velocity centrifugations, the latter two on sucrose gradients, yielded fractions S2, I3, P4, and P5. The yield of patches was not affected by addition of 5 μM phalloidin, 2 mM MgCl<sub>2</sub>, or 1 mM EGTA.

Patches were stable even when purified without chemical cross-linker treatment. To determine if patch stability resulted from a balance of actin polymerization and depolymerization, we added 20 μM latrunculin A to fraction P4, at a 10<sup>8</sup> M excess to actin subunits. The number and intensity of GFP-labeled patches did not change over 16 h at 4°C. Also, we induced patches to disassemble over ~2 h by raising the temperature to 25°C and measured the number and fluorescence intensity of GFP-labeled patches with or without 4 μM latrunculin. Latrunculin did not affect the rate of patch disassembly, indicating that in the conditions of our protocol, even in the absence of cross-linker, actin patches

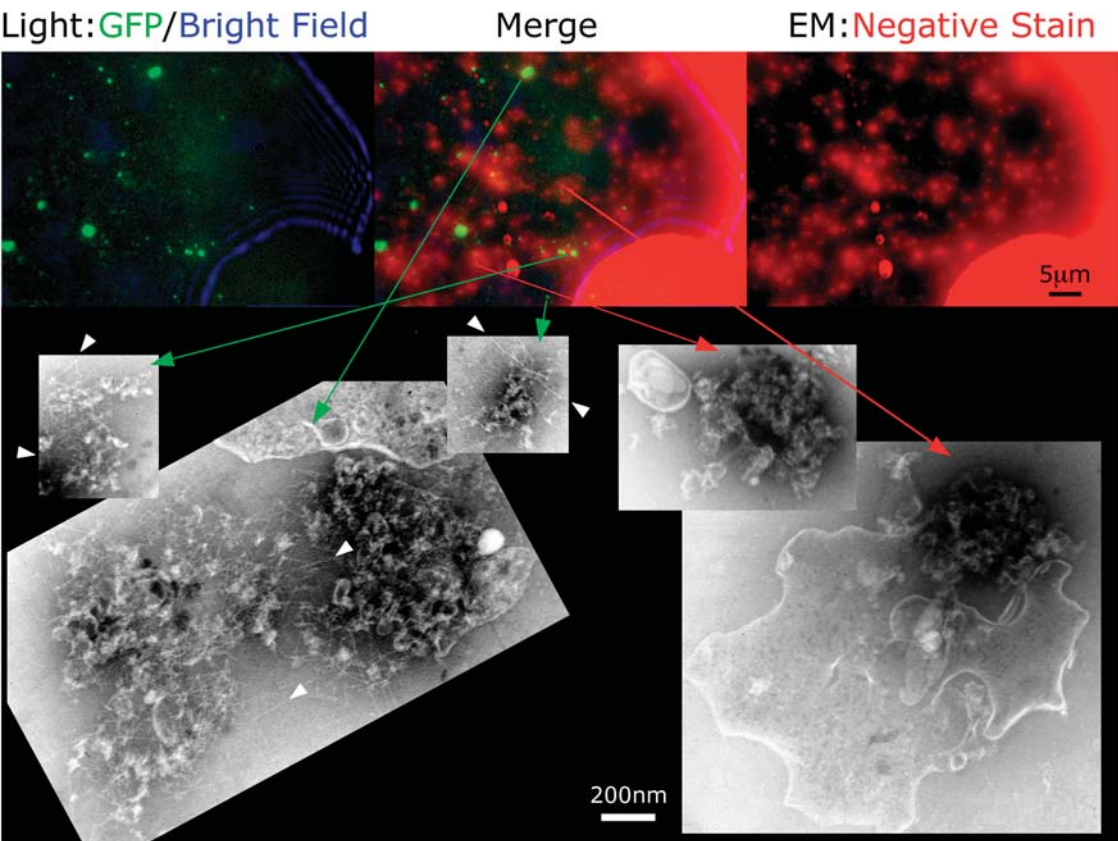


Figure 2. **Correlation of light and electron microscope images.** The top portion shows GFP fluorescence (green) and bright field (blue) light microscope images of an EM grid coated with an actin patch preparation, overlaid on a colorized (red) low magnification EM image after processing the grid by negative staining. The large red area outlined by the blue diffraction pattern is the grid's copper lattice. The bottom portion shows EMs of structures that do or do not contain GFP. A meshwork of branched filaments is seen in GFP-containing structures. Some filaments are indicated by arrowheads. Structures lacking GFP always contained proteinaceous aggregates, sometimes membranes, but never filaments. Strain YJC1453.

were not dynamic or turning over. Patches did disassemble if removed from high osmolarity or cold temperature.

To assess the purification, we performed SDS-PAGE on fractions of a purification performed without chemical cross-linker. Coomassie-stained protein profiles of lysed cells, cleared lysate, and all fractions up to I3 were indistinguishable. Actin was the most prominent band in P5, a substantial enrichment. However, most of the P5 bands were also present in I3, showing that the purification was only partial (Fig. 1 E). We also counted the number of GFP-labeled patches and examined the relative amount of actin

with Western blots. Actin cofractionated with GFP-labeled patches except for the presence of some actin, presumably free monomers, in the supernatant above fraction I3. The number of Cap1-GFP labeled patches and the amount of actin were enriched ~50-fold and >300-fold, respectively, relative to fraction S1 (Table I). Abp1-GFP was lost from patches to a greater degree than was Cap1-GFP. The enrichment of GFP-labeled patches was significantly higher in cross-linked preparations, although SDS-PAGE and immunoblot analysis of these samples were not possible.

Identification of actin patches in the EM

Even with chemical cross-linker, actin patches were only partially purified, so we needed to identify patches in the EM. We adhered GFP-labeled patches to an EM grid and examined the grid by fluorescence microscopy. The same grid was negative-stained and examined in the EM. Fiducial marks, including grid bars, were used to align brightfield and fluorescence images with low magnification EM images, allowing one to identify GFP-labeled patches unambiguously. Every GFP-labeled patch coincided with a structure in the EM, but only ~10% of negatively stained objects contained GFP (Fig. 2).

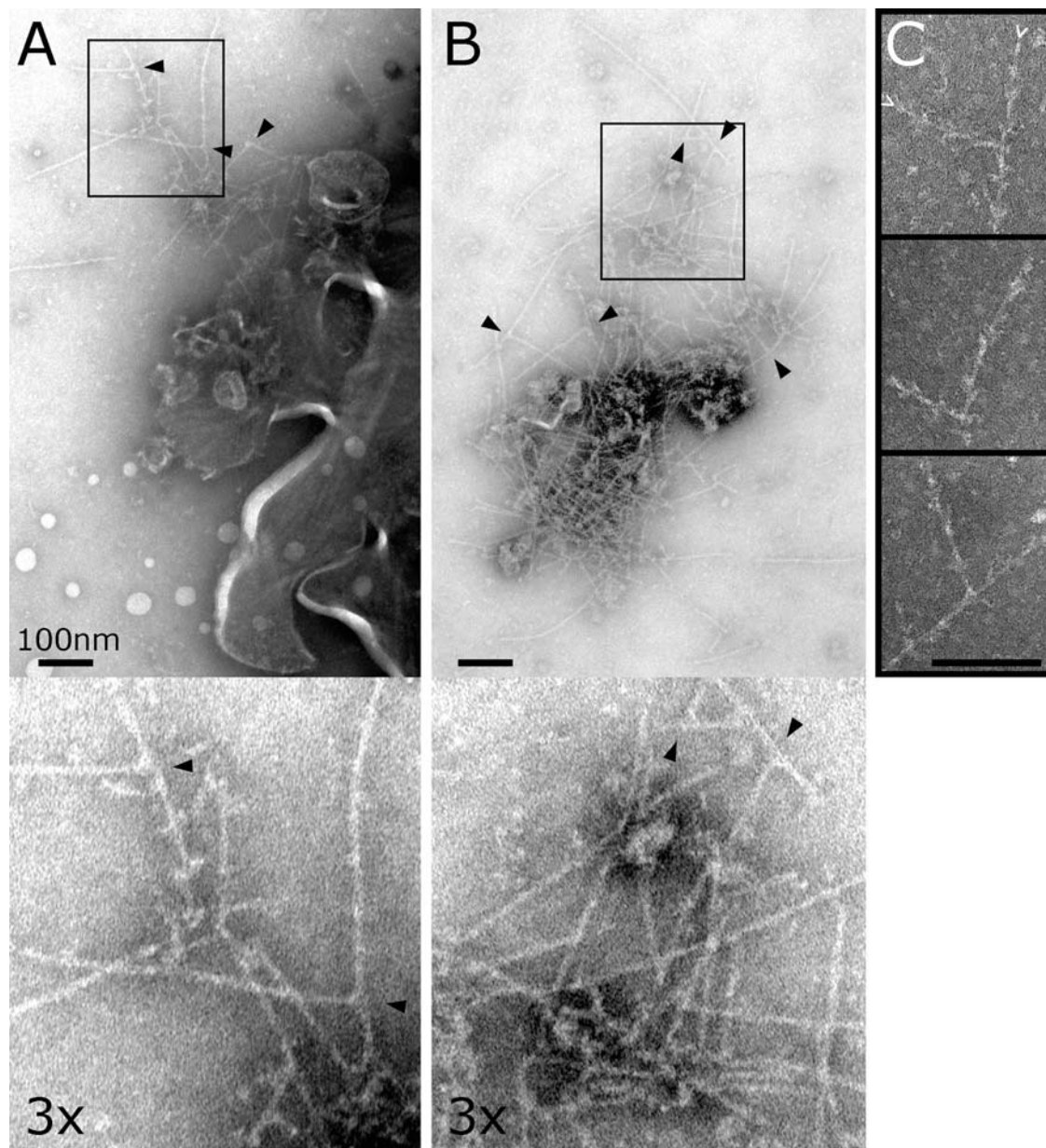
Actin patches from chemically cross-linked preparations contained branched networks of thin filaments resembling

Table I. **Enrichment of actin patches during purification**

	Total protein	Green patches		Actin	
	mg, mean ± SD, n ≥ 3	% of S1	–Fold Enrichment	% of S1	–Fold Enrichment
S1	36 ± 9	100	1	100	1
I3	6.7 ± 3.7	90	4.8	50	2.7
P4	0.110 ± 0.017	20	65	44	144
P5	0.037 ± 0.016	5	49	38	370

Fractions from samples purified without cross-linking were assayed for total protein, number of Cap1-GFP patches by fluorescence microscopy, and relative amount of actin by immunoblot. Enrichment is relative to the cleared lysate (S1). The strain was YJC1453.





**Figure 3. Actin patches from preparations lacking cross-linker, with S1 decoration.** Actin patches prepared without cross-linking were treated briefly with latrunculin A, exposing filamentous networks. Most patches were associated with membranes (A); others were not (B). Arrowheads mark some end to side branches. (C) Myosin S1 decoration. Strain YJC1453.

actin. The correlation between filament networks and fluorescent patches was very good. In areas where the negative stain allowed filament visualization, >95% of fluorescent patches coincided with filament networks, and >90% of thin filament networks coincided with a fluorescent patch. In addition, the fluorescence intensity correlated with filament network size. Often, proteinaceous material obscured the filaments in a portion of a patch (Fig. 2).

Filaments were less apparent in actin patch preparations purified without chemical cross-linking, even considering the lower yield of patches. These putative patches were predominantly membranous and proteinaceous with a few thin filaments at their periphery. Neither 0.1% Triton X-100 nor 1 M NaCl treatment increased the appearance of filaments substantially. However, addition of 50  $\mu$ M latrunculin A for

5 min at 25°C, followed by fixation, did produce filamentous networks (Fig. 3). This result is quite surprising, and we do not have a compelling explanation for why latrunculin should have this effect. However, new polymerization should not occur in the presence of latrunculin. Thus, the branched filaments must have been present before the treatment. We do not know if latrunculin affected the network's organization.

Most filament networks in latrunculin-treated preparations were associated with 1–3  $\mu$ m membranous structures (Fig. 3). In the absence of cross-linker, addition of 0.1–10% Triton X-100 to cell lysate did not affect GFP-labeled patches; however, patches disappeared when the lysate was centrifuged. Thus, membrane may stabilize some patches to centrifugations. These are a minority of patches because

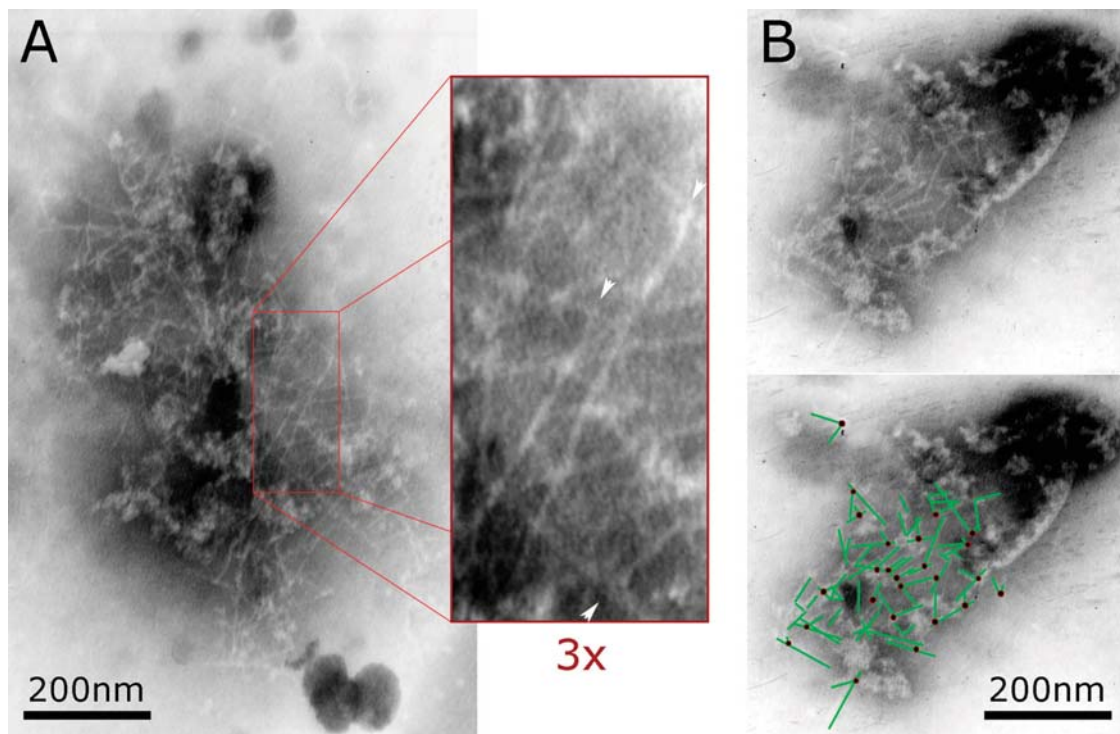


Figure 4. **Actin patches from cross-linked preparations.** (A) The branched filament network of a typical actin patch. Arrowheads mark some branches. (B) A graphical representation (bottom) of the actin filaments in another typical patch (top). Filament length and branching were quantitated for this patch, as indicated by the green lines and red dots, respectively. Strain YJC1453.

cross-linked preparations contained many more fluorescent patches, and few cross-linked patches were associated with membranes in the EM.

### S1 decoration and the branching pattern of actin patch filaments

We decorated filaments with myosin S1. The patches could not be chemically cross-linked for S1 binding, so latrunculin treatment was used, as described above. The filaments were decorated in a chevron pattern characteristic of actin. At every end to side branch, the daughter filament's barbed end projected away from the branch point (Fig. 3 C). The angle between the daughter filament and the mother filament segment with the barbed end was  $69 \pm 8^\circ$  (mean  $\pm$  SD,  $n = 18$ ), the same as  $70 \pm 7^\circ$  for branches seen with purified Arp2/3 complex (Mullins et al., 1998; Volkmann et al., 2001). Lamellipodia of vertebrate cells contain Arp2/3 complex branches with barbed ends oriented toward the leading edge (Svitkina and Borisy, 1999). The branched filaments in our yeast actin patches showed no linear or radial directionality; the network was isotropic. Negative staining flattens the specimen, so some architectural features may have been lost.

In 11 patches from a cross-linked preparation, patch diameter was  $409 \pm 170$  nm (mean  $\pm$  SD; range, 150–750), the number of filaments per patch was  $85 \pm 46$  (mean  $\pm$  SD; range, 18–174), the number of end to side branches per patch was  $29 \pm 16$  (mean  $\pm$  SD; range, 7–57), and the average filament length was  $50 \pm 27$  nm (mean  $\pm$  SD;  $n = 938$ ; range, 10–195). A representative analysis of one patch is shown in Fig. 4. The short filament length and degree of

branching supports the notion that Arp2/3-based nucleation activity in patches is present as indicated by studies of Arp2/3 mutants (Winter et al., 1997).

We looked for evidence of different populations of patches. In lamellipodia, filaments become longer and less branched over time (Svitkina and Borisy, 1999) so older patches might have longer or less branched filaments. However, the average filament length was uniform (Fig. S2, available at <http://www.jcb.org/cgi/content/full/jcb.200404159/DC1>), and filament architecture was similar in all patches. Patch diameter, number of filaments, and number of branches correlated significantly (Fig. S2). Thus, patches differed only in size, containing different amounts of branched filament network.

The daughter was more often attached near the middle of the mother filament; 51% of branches were in the middle third of the mother filament, whereas 24–25% occurred in each distal third ( $n = 91$ ,  $P < 0.1$  by  $\chi^2$ ). The daughter filament length was  $66 \pm 38\%$  of the entire length of its mother filament.

### Analysis of mutant patches

Yeast Sac6/fimbrin bundles actin filaments in vitro, localizes to patches in vivo, and is present at a 1:10 molar ratio with actin (Goodman et al., 2003). However, bundles were not seen in patches from wild-type cells. Purified yeast Sac6/fimbrin also stabilizes actin filaments against depolymerization (Goode et al., 1999), and *sac6Δ* mutant strains have synthetic defects with many actin-regulating proteins (Goodman et al., 2003). Therefore, we asked if Sac6 was important for patch



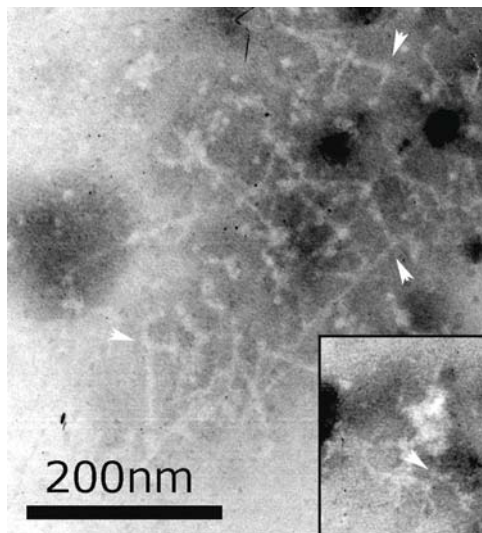


**Figure 5. Cross-linked actin patches lacking Sac6/fimbrin.** One of the larger patches from a *sac6Δ* strain, YJC3580. Most patches were far smaller (inset). Arrowheads mark some branches.

stability and integrity by purifying and studying patches from a strain lacking Sac6/fimbrin. Actin patches from a *sac6* null strain disassembled within 20 min of cell lysis in the absence of chemical cross-linker, even in the presence of 1 M sorbitol. Wild-type patches were stable for >24 h under these conditions. Even *sac6Δ* patches cross-linked within 5 min of cell lysis were significantly dimmer than patches in vivo. We identified purified *sac6Δ* patches, or patch fragments, in the EM by correlation microscopy. They were smaller in diameter (70–290 nm,  $n = 10$ ) than wild-type patches (150–750 nm) with proportionately fewer filaments and branches. However, the density and architecture of the network was normal (Fig. 5). Therefore, Sac6/fimbrin is important for patch stability, possibly stabilizing filaments by side-binding, but is not essential for the general architecture.

Capping protein has a central role in the dendritic nucleation model, localizes to actin patches in yeast (Kim et al., 2004), and increases branching by Arp2/3 complex in actin polymerization reactions in vitro (Blanchoin et al., 2000). Unexpectedly, actin patches purified from a *cap1* null strain, with Sac6-GFP, showed a qualitatively normal organization of actin filaments, including filament length and branching, relative to wild-type patches.

### The dendritic nucleation model and yeast actin patches

The dendritic nucleation model applies only in part to the assembly and motility of yeast actin patches. The model predicts a highly branched filament network with branches characteristic of Arp2/3 complex, which we observed here. The model is also supported by previous studies showing Arp2/3's importance for patch assembly and motility (Winter et al., 1997). On the other hand, the model predicts an important role for capping protein, and the filament architecture of patches lacking capping protein was normal here. Moreover, capping protein and cofilin are not necessary for normal patch movement in vivo (Lappalainen and Drubin, 1997; Kim et al., 2004). Perhaps yeast cytoplasm in general

lacks free barbed ends that must be capped to “funnel” actin polymerization to the patch. Indeed, free barbed ends are detected only at actin patches in permeabilized cell assays (Li et al., 1995; Kim et al., 2004).

## Materials and methods

### Yeast strains

Cap1-GFP was expressed in the *MATa* Research Genetics/Invitrogen S288C background (BY4742, *his3Δ ura3Δ leu2Δ met15Δ*), by integrating *GFP* at the 3' end of the *CAP1* locus, as described previously (Karpova et al., 1998), resulting in strain YJC2718. The Cap1-GFP fusion rescues the actin patch depolarization phenotype of a *cap1Δ* strain. YJC2718 was crossed with the Research Genetics/Invitrogen *MATa sac6Δ* strain (record number 14063), sporulated, and tetrad dissected, resulting in the strain YJC3580 (*MATa CAP1-GFP-HIS3 sac6Δ::KanR his3Δ ura3Δ leu2Δ*). The presence of Cap1-GFP was verified visually by fluorescence microscopy as well as by PCR across the junction of *CAP1* and *GFP*. The *sac6Δ* disruption was confirmed by sequencing the upstream tag. A haploid *cap1Δ* Sac6-GFP strain, YJC3481 (*MATa SAC6-GFP-HIS3 cap1Δ::KanR his3Δ ura3Δ leu2Δ lys2Δ*), and a homozygous diploid *CAP1-GFP* strain, YJC1453 (*MATa/α CAP1-GFP-HIS3/CAP1-GFP-HIS3 his3/his3 ura3/ura3 leu2/leu2*), were described previously (Karpova et al., 2000; Kim et al., 2004).

### Actin patch purification

Yeast were grown in 1 liter of YPD to an  $OD_{600}$  of ~1.0. Cells were washed twice with KS (200 mM potassium phosphate, pH 7.0, 1 M sorbitol), suspended in 1 ml KS, 0.1 M  $\beta$ -mercaptoethanol, and 0.6 mg/ml zymolyase 20T (ICN Biomedicals), and incubated for 1 h at 37°C. Spheroplasts were washed twice with KS, suspended in 1 ml of 2% Mega-9 nonionic detergent (Calbiochem) in low sorbitol (0.5 M) KS, with 2 mM PMSF, 2 mM benzamide, 20  $\mu$ g/ml leupeptin, and 20  $\mu$ g/ml pepstatin A. 10–12 titrations with a 0.46-mm bore 200  $\mu$ l pipet (Rainin) were performed. Further steps were performed at 4°C. The lysate was cleared by a 10-min microfuge centrifugation, yielding fraction S1. In some experiments, 0.1% glutaraldehyde was added to S1 for 10 min and quenched with 0.2 M ammonium acetate. S1 was centrifuged 10 min at 70,000 rpm in a TL100.1 rotor in an ultracentrifuge (model Optima TL; Beckman Coulter). The supernatant S2 was collected, avoiding lipid at the meniscus, layered on 100  $\mu$ l KS pads, and centrifuged in the same way for 30 min. The bottom ~150  $\mu$ l from each tube, fraction I3, was mixed 1:1 with KS, loaded onto a 10 ml 5–20% sucrose gradient in KS, and centrifuged 2.5 h at 30,000 rpm in a SW-41 rotor. The bottom 100–200  $\mu$ l, fraction P4, was mixed 1:1 with 0.2 M potassium phosphate, pH 7.0, and centrifuged on a sucrose gradient as before. The bottom 100–200  $\mu$ l, fraction P5, was diluted 1:1 with 0.2 M potassium phosphate, pH 7.0, stored on ice, and used within 24 h. P5 was microfuged for 3 min before use.

### Negative stain EM

Glow-discharged formvar-coated copper grids were placed onto 30  $\mu$ l of sample for 5–10 min. In some experiments the grids were moved to 50  $\mu$ M latrunculin A, 2.5% DMSO in KS for 5 min. Grids were moved rapidly through two drops of KS, into 1% glutaraldehyde in KS. After 5–10 min grids were moved through four drops each of KS, 40  $\mu$ g/ml bacitracin, and 0.02  $\mu$ M filtered 3% phosphotungstic acid. Excess liquid was blotted, and dried grids were viewed on a JEOL-1200EX electron microscope at 80–90 kV (Lewis and Bridgman, 1992).

### Fluorescence microscopy and correlation of images

GFP-labeled actin patches were viewed in whole yeast and cell extracts using a HiQ FITC filter cube and a cooled CCD camera as described previously (Karpova et al., 2000). Cell lysates and spheroplasts were stained with 660 nM rhodamine-phalloidin (Fluka) after fixation with 0.1% glutaraldehyde, and the spheroplasts were permeabilized with 0.1% Triton X-100. Fluorescence intensity was quantitated with NIH Image.

For correlation microscopy, EM grids with GFP-labeled patches were immersed in KS and placed between a slide and coverslip. Excess liquid was wicked away. Bright field and fluorescence images were taken. To avoid damaging the formvar grid, we only brought the objective close enough to focus, and we did not move the specimen while in focus. Cumulative fluorescence exposure was limited to 5 s to avoid background fluorescence from formvar. Coverslips and grids were floated off slides with KS, and the grids were gently blotted and processed for negative stain EM.

Light and EM fields were correlated with London finder grids or imperfections in standard grids (Electron Microscopy Sciences). Low magnification,  $\sim 1500\times$ , EM images were aligned with the light images in Adobe Photoshop. Multiple patches were identified in the EM within  $1\text{--}2\ \mu\text{m}$  of their predicted location, leading to a refined alignment at a precision of  $100\text{--}200\ \text{nm}$  over the entire  $\sim 40 \times 60\ \mu\text{m}$  field. Patches from haploid and diploid strains were similar.

### Online supplemental material

Online supplemental material includes protein methods and two figures. Fig. S1 shows actin depolymerization after dilution into KS or other buffers. Fig. S2 shows which actin patch characteristics are correlated. Online supplemental material is available at <http://www.jcb.org/cgi/content/full/jcb.200404159/DC1>.

We thank Christopher Mills, Darcy Moschenross, and Margaret van Bakergem for technical assistance, Dr. T. Karpova for advice and preliminary experiments, G. Phillips for EM assistance, and Drs. A. Rodal, B. Goode, D. Drubin, and J. Hartwig for sharing unpublished results critical for understanding our results.

This work was supported by National Institutes of Health grants GM47337 to J.A. Cooper and NS26150 to P.C. Bridgman, and American Heart Association predoctoral fellowship 3225 38972 to M.E. Young.

Submitted: 27 April 2004

Accepted: 12 July 2004

## References

- Adams, A.E.M., and J.R. Pringle. 1984. Relationship of actin and tubulin distribution to bud growth in wild-type and morphogenetic-mutant *Saccharomyces cerevisiae*. *J. Cell Biol.* 98:934–945.
- Blanchoin, L., K.J. Amann, H.N. Higgs, J.B. Marchand, D.A. Kaiser, and T.D. Pollard. 2000. Direct observation of dendritic actin filament networks nucleated by Arp2/3 complex and WASP/Scar proteins. *Nature*. 404:1007–1011.
- Cameron, L.A., T.M. Svitkina, D. Vignjevic, J.A. Theriot, and G.G. Borisy. 2001. Dendritic organization of actin comet tails. *Curr. Biol.* 11:130–135.
- Goode, B.L., J.J. Wong, A.C. Butty, M. Peter, A.L. McCormack, J.R. Yates, D.G. Drubin, and G. Barnes. 1999. Coronin promotes the rapid assembly and cross-linking of actin filaments and may link the actin and microtubule cytoskeletons in yeast. *J. Cell Biol.* 144:83–98.
- Goodman, A., B.L. Goode, P. Matsudaira, and G.R. Fink. 2003. The *Saccharomyces cerevisiae* calponin/transgelin homolog Scp1 functions with fimbrin to regulate stability and organization of the actin cytoskeleton. *Mol. Biol. Cell*. 14:2617–2629.
- Kaksonen, M., Y. Sun, and D.G. Drubin. 2003. A pathway for association of receptors, adaptors, and actin during endocytic internalization. *Cell*. 115:475–487.
- Karpova, T.S., S.L. Moltz, L.E. Riles, U. Guedener, J.H. Hegemann, S. Veronneau, H. Bussey, and J.A. Cooper. 1998. Depolarization of the actin cytoskeleton is a specific phenotype in *Saccharomyces cerevisiae*. *J. Cell Sci.* 111:2689–2696.
- Karpova, T.S., S.L. Reck-Peterson, N.B. Elkind, M.S. Mooseker, P.J. Novick, and J.A. Cooper. 2000. Role of actin and Myo2p in polarized secretion and growth of *Saccharomyces cerevisiae*. *Mol. Biol. Cell*. 11:1727–1737.
- Kim, K., A. Yamashita, M.A. Wear, Y. Maeda, and J.A. Cooper. 2004. Capping protein binding to actin in yeast: biochemical mechanism and physiological relevance. *J. Cell Biol.* 164:567–580.
- Lappalainen, P., and D.G. Drubin. 1997. Cofilin promotes rapid actin filament turnover in vivo. *Nature*. 388:78–82.
- Lewis, A.K., and P.C. Bridgman. 1992. Nerve growth cone lamellipodia contain two populations of actin filaments that differ in organization and polarity. *J. Cell Biol.* 119:1219–1243.
- Li, R., Y. Zheng, and D.G. Drubin. 1995. Regulation of cortical actin cytoskeleton assembly during polarized cell growth in budding yeast. *J. Cell Biol.* 128:599–615.
- Loisel, T.P., R. Boujemaa, D. Pantaloni, and M.F. Carlier. 1999. Reconstitution of actin-based motility of *Listeria* and *Shigella* using pure proteins. *Nature*. 401:613–616.
- Medalia, O., I. Weber, A.S. Frangakis, D. Nicastro, G. Gerisch, and W. Baumeister. 2002. Macromolecular architecture in eukaryotic cells visualized by cryoelectron tomography. *Science*. 298:1209–1213.
- Mulholland, J., D. Preuss, A. Moon, A. Wong, D. Drubin, and D. Botstein. 1994. Ultrastructure of the yeast actin cytoskeleton and its association with the plasma membrane. *J. Cell Biol.* 125:381–391.
- Mullins, R.D., J.A. Heuser, and T.D. Pollard. 1998. The interaction of Arp2/3 complex with actin: Nucleation, high affinity pointed end capping, and formation of branching networks of filaments. *Proc. Natl. Acad. Sci. USA*. 95:6181–6186.
- Nefsky, B., and A. Bretscher. 1992. Yeast actin is relatively well behaved. *Eur. J. Biochem.* 206:949–955.
- Pollard, T.D., and G.G. Borisy. 2003. Cellular motility driven by assembly and disassembly of actin filaments. *Cell*. 112:453–465.
- Svitkina, T.M., and G.G. Borisy. 1999. Arp2/3 complex and actin depolymerizing factor cofilin in dendritic organization and treadmilling of actin filament array in lamellipodia. *J. Cell Biol.* 145:1009–1026.
- Utsugi, T., M. Minemura, A. Hirata, M. Abe, D. Watanabe, and Y. Ohya. 2002. Movement of yeast 1,3-beta-glucan synthase is essential for uniform cell wall synthesis. *Genes Cells*. 7:1–9.
- Volkman, N., K.J. Amann, S. Stoilova-McPhie, C. Egile, D.C. Winter, L. Hazelwood, J.E. Heuser, R. Li, T.D. Pollard, and D. Hanein. 2001. Structure of Arp2/3 complex in its activated state and in actin filament branch junctions. *Science*. 293:2456–2459.
- Wear, M., and J. Cooper. 2004. Capping protein: new insights into mechanism and regulation. *Trends Biochem. Sci.* 29:418–428.
- Winter, D., A.V. Podtelebnikov, M. Mann, and R. Li. 1997. The complex containing actin-related proteins Arp2 and Arp3 is required for the motility and integrity of yeast actin patches. *Curr. Biol.* 7:519–529.